Electronic Supplementary Information

Plasmon-Enhanced Photothermal Properties of Au@$Ti_3C_2T_x$ Nanosheets for Antibacterial Applications

Shiqi Wen,[a,b,1] Youlin Xiong,[a,1] Shuangfei Cai,[a,*] Haolin Li,[a,b] Xining Zhang,[a,b] Qian Sun,[a] Rong Yang[a,b,*]

[a] CAS Key Lab for Biomedical Effects of Nanomaterials and Nanosafety, Center of Materials Science and Optoelectronics Engineering, CAS center for Excellence in Nanoscience, National Center for Nanoscience and Technology, University of Chinese Academy of Sciences, Beijing 100190, China
[b] Sino-Danish College, Sino-Danish Center for Education and Research, University of Chinese Academy of Sciences, Beijing 100190, China
[1] These authors contributed equally to this work.

*Corresponding authors. E-mail addresses: caisf@nanoctr.cn, yangr@nanoctr.cn

Contents

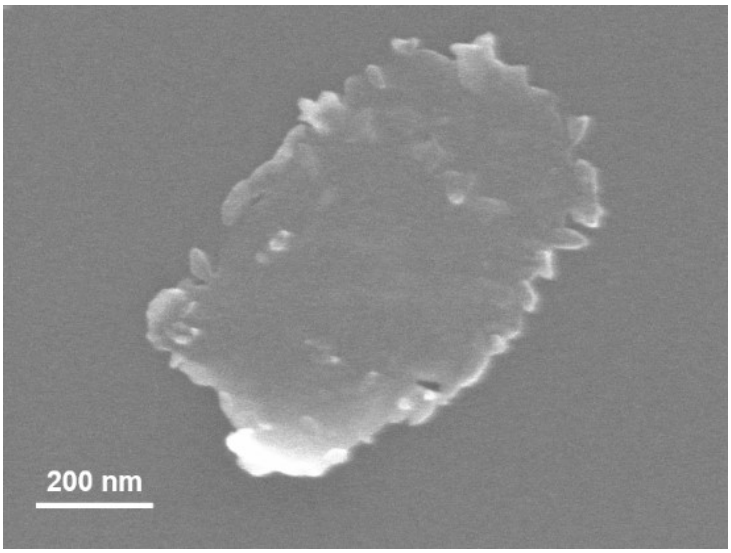

Figure S1. SEM image of the $Ti_3C_2T_x$ NSs.

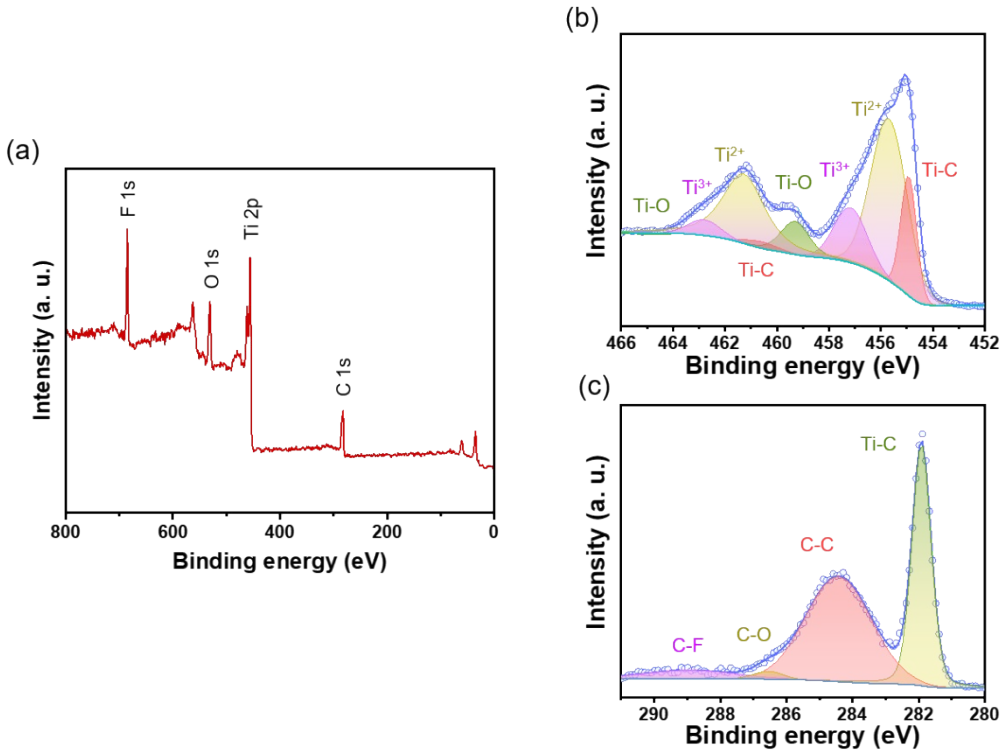

Figure S2. XPS analysis of the $Ti_3C_2T_x$ NSs. (a) XPS survey spectrum. (b) High-resolution peak-fitting XPS spectrum of the Ti 2p region. (c) High-resolution peak-fitting XPS spectrum of the C 1s region.

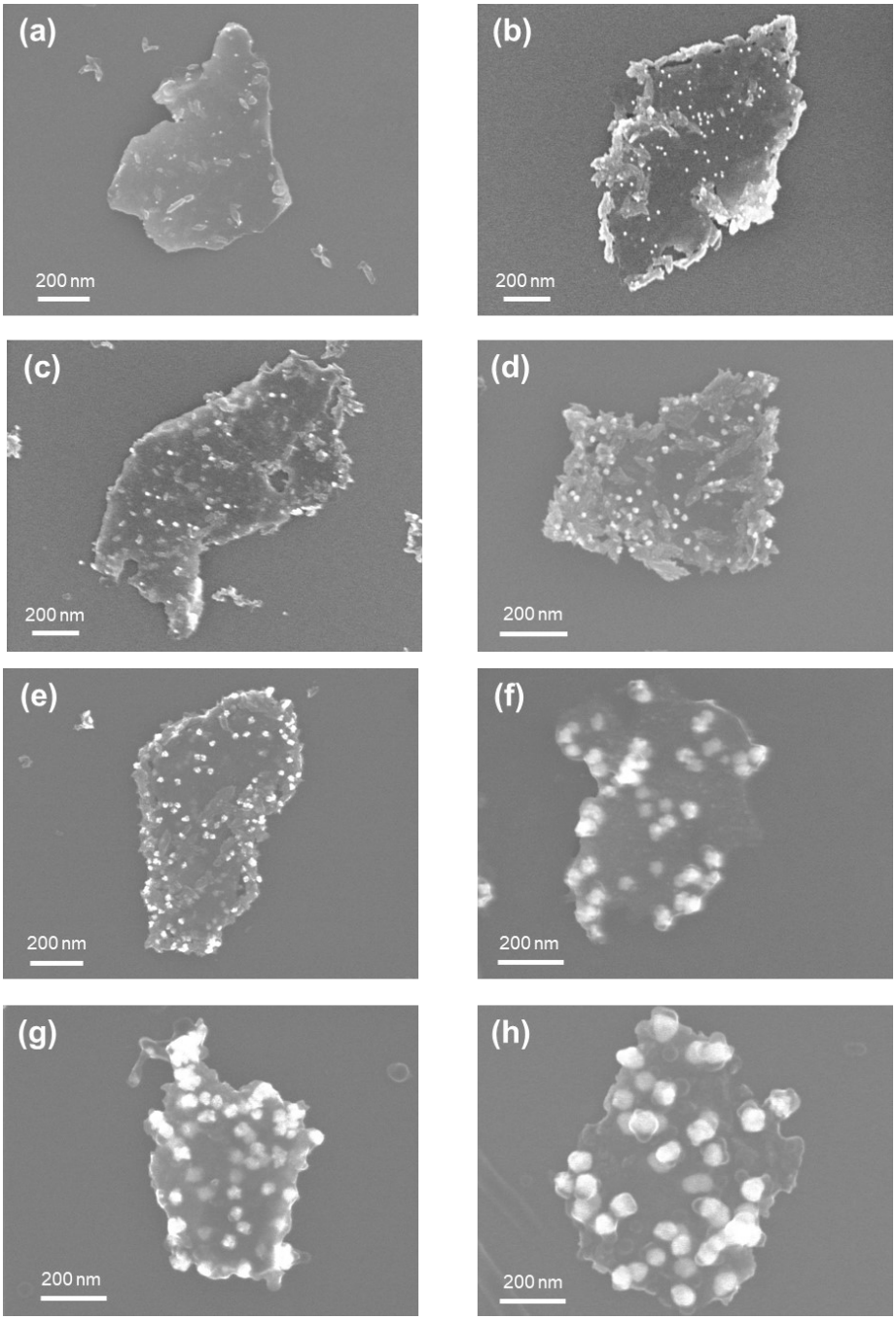

Figure S3. SEM images of the $Au_y@Ti_3C_2T_x$ nanocomposites with different Au/Ti feeding ratios: (a) 0.0017, (b) 0.0042, (c) 0.0085, (d) 0.017, (e) 0.034, (f) 0.068, (g) 0.136, and (h) 0.2.

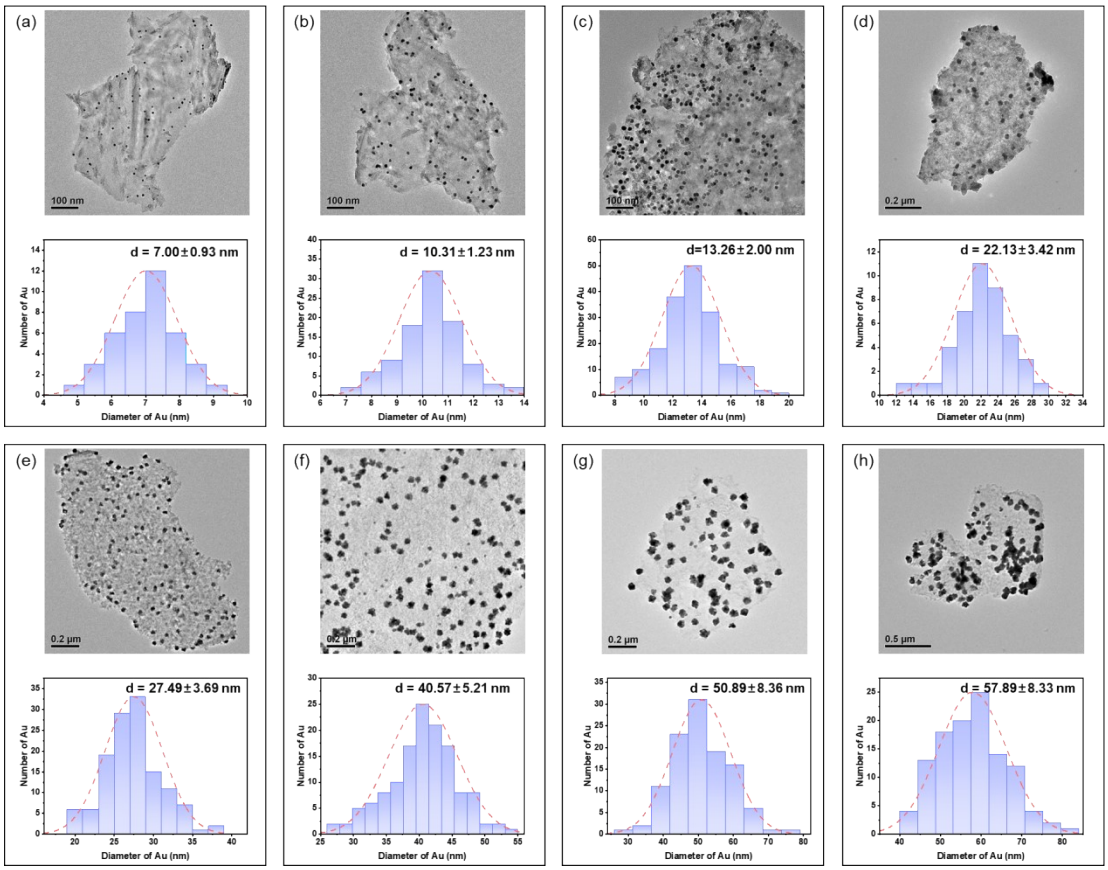

Figure S4. TEM images of the $Au_y@Ti_3C_2T_x$ nanocomposites and size distribution histograms of the Au NPs obtained by different Au/Ti feeding ratios: (a) 0.0017, (b) 0.0042, (c) 0.0085, (d) 0.017, (e) 0.034, (f) 0.068, (g) 0.136, and (h) 0.2.

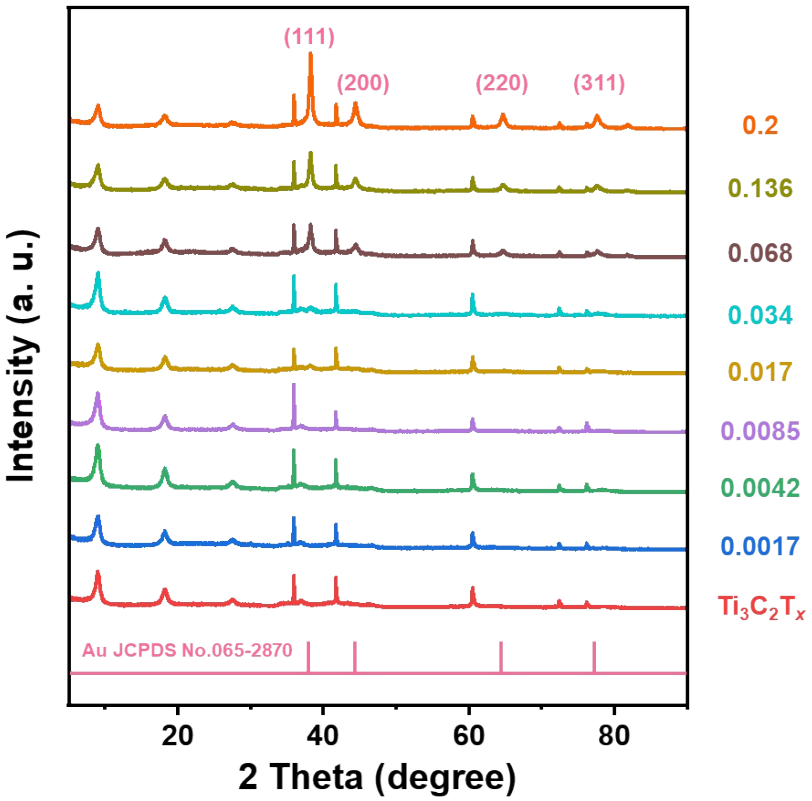

Figure S5. XRD patterns of the $Au_y@Ti_3C_2T_x$ nanocomposites obtained by different Au/Ti feeding ratios.

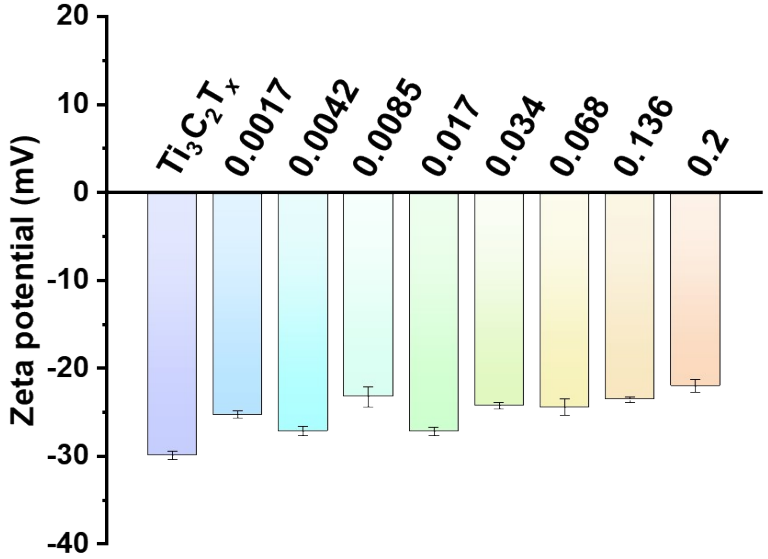

Figure S6. Zeta potential of the $Au_y@Ti_3C_2T_x$ nanocomposites obtained by different Au/Ti feeding ratios.

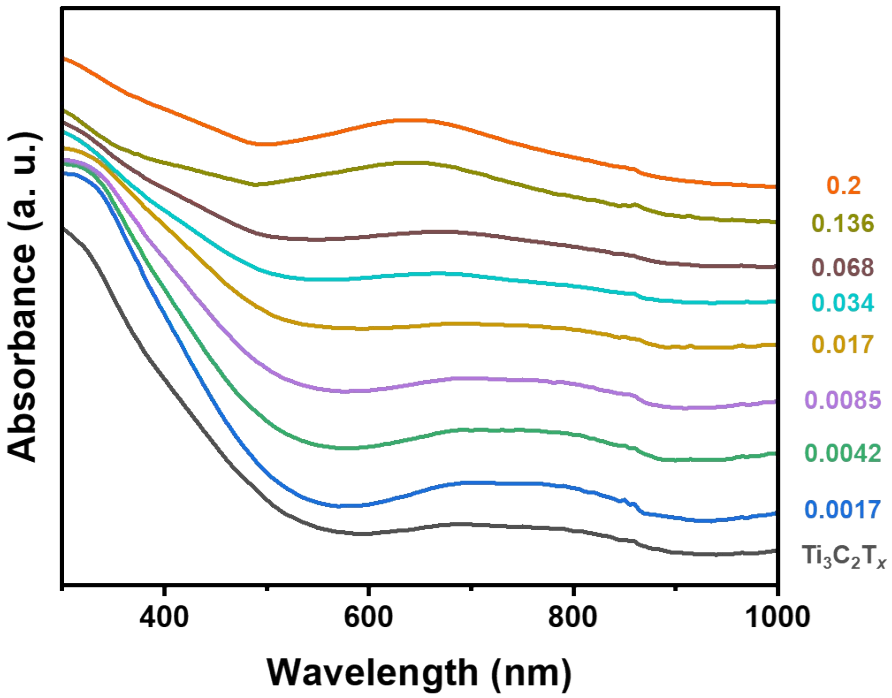

Figure S7. UV-Vis-NIR absorption spectra of the $Au_y@Ti_3C_2T_x$ nanocomposites obtained by different Au/Ti feeding ratios.

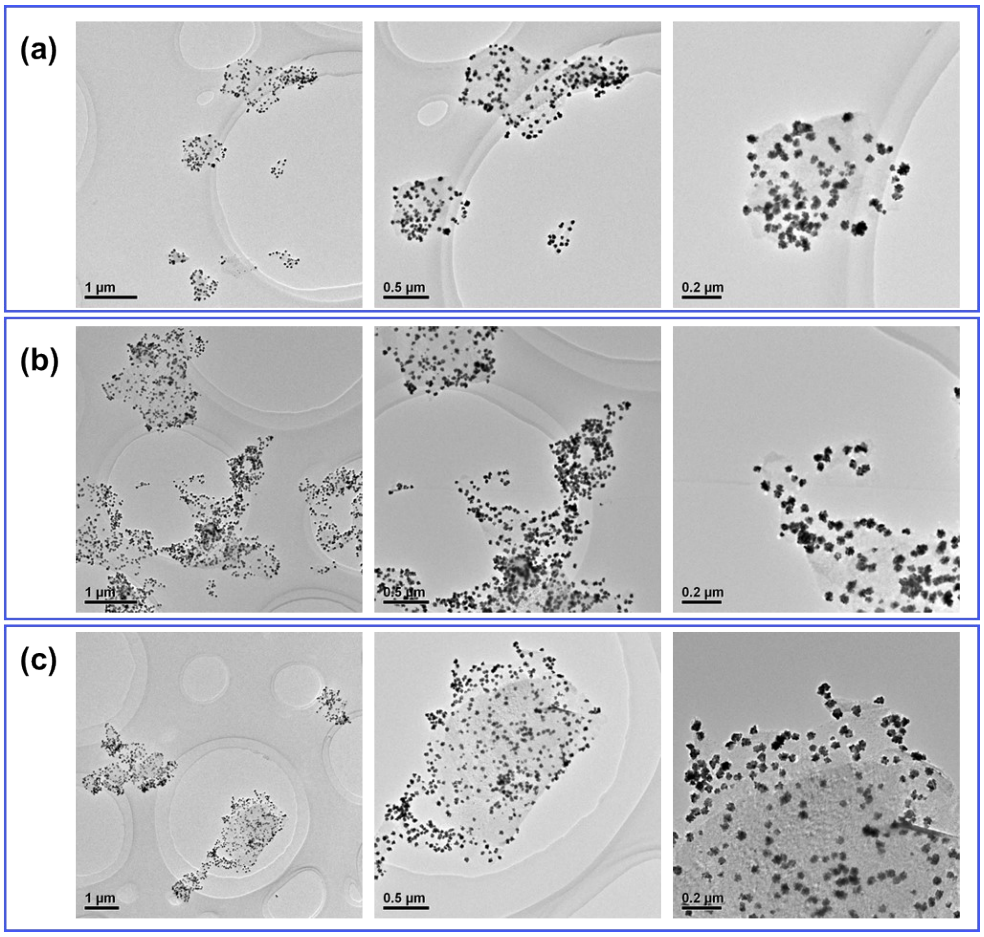

Figure S8. TEM images of the $Au_{0.017}@Ti_3C_2T_x$ nanocomposites during three washing/centrifugation cycles: (a) first, (b) second, (c) third cycle.

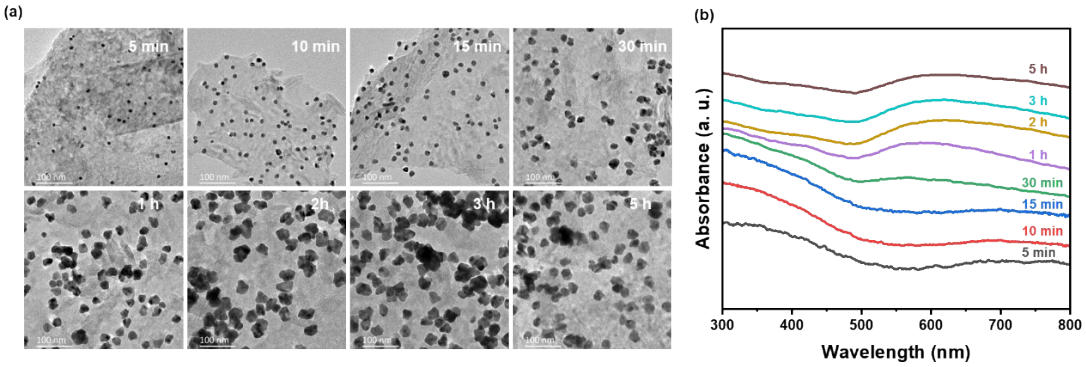

Figure S9. Characterization of the intermediates collected from different reaction time during the synthesis of $Au_{0.027}@Ti_3C_2T_x$. (a) TEM images. (b) Corresponding UV-Vis spectra.

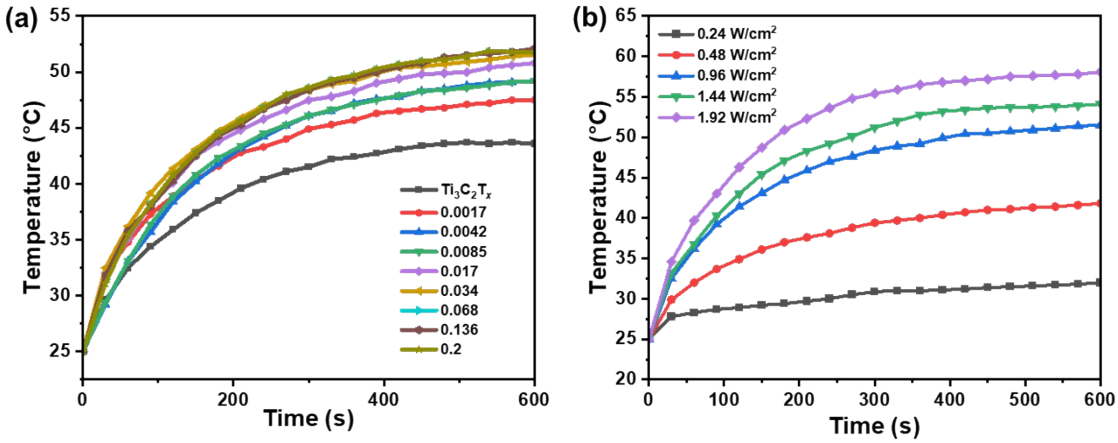

Figure S10. The photothermal activity test of the $Au_y@Ti_3C_2T_x$ nanocomposites (100 μg/mL) obtained by different Au/Ti feeding ratios. (a) Effect of the Au composition on the variation in the temperature. (b) Effect of the power density on the variation in the temperature using the $Au_{0.017}@Ti_3C_2T_x$ under a 660 nm laser.

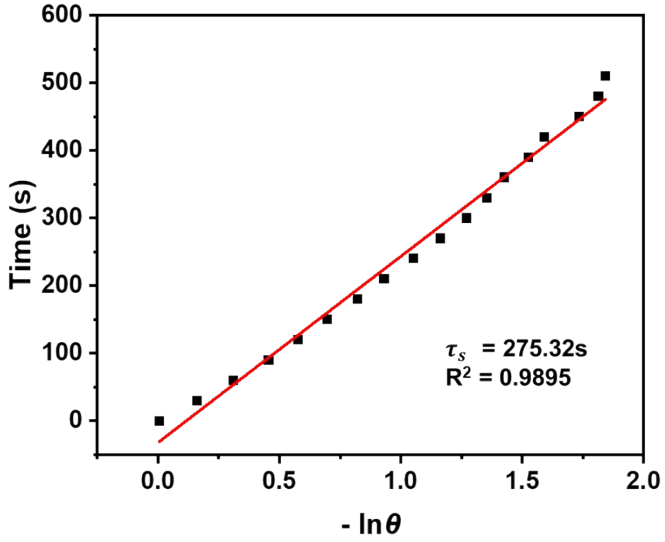

Figure S11. The fitting line of experimental data of time *vs.* -lnθ obtained from the cooling period for the $Ti_3C_2T_x$ NSs.

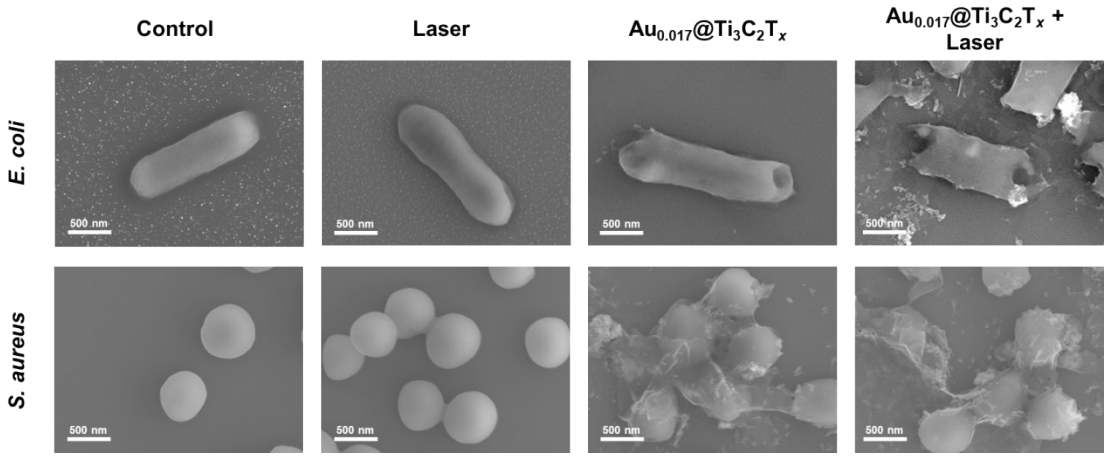

Figure S12. SEM images with higher magnification of E. *coli* (top panel) and S. *aureus* (bottom panel) treated with control, laser (660 nm, 0.96 W/cm^2), $Au_{0.017}@Ti_3C_2T_x$ (50 μg/mL), and laser + $Au_{0.017}@Ti_3C_2T_x$.

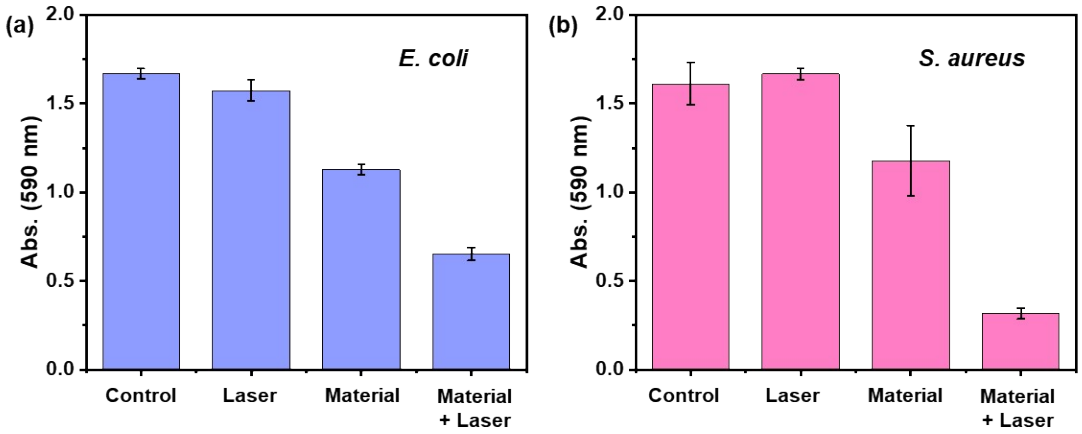

Figure S13. Biofilm elimination of (a) *E. coli* and (b) *S. aureus* under different treatments: control, laser (660 nm, 1.92 W/cm^2, 20 min), $Au_{0.017}@Ti_3C_2T_x$ (100 μg/mL), and laser + $Au_{0.017}@Ti_3C_2T_x$.

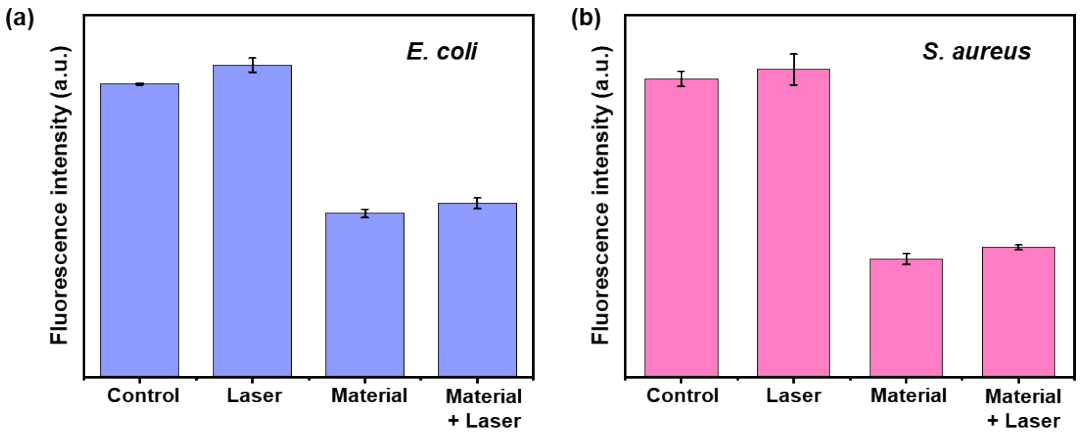

Figure S14. Intracellular ROS level in (a) *E. coli,* (b) *S. aureus* treated with control, laser (660 nm, 0.96 W/cm^2), $Au_{0.017}@Ti_3C_2T_x$ (50 μg/mL), and laser + $Au_{0.017}@Ti_3C_2T_x$.

Table S1. The composition of Au in the $Au_y@Ti_3C_2T_x$ nanocomposites

Entry	Feeding ratio of Au/Ti	Analyzed ratio of Au/Ti
1	0.0017	0.0007
2	0.0042	0.0014
3	0.0085	0.0024
4	0.017	0.0072
5	0.034	0.017
6	0.068	0.027
7	0.136	0.062
8	0.2	0.098

Appendix: Calculation of the photothermal conversion efficiency (PCE)[1]

The total energy balance of the system can be expressed as

$$\sum_i m_i C_{p,i} \frac{dT}{dt} = Q_{\text{Material}} + Q_{\text{Dis}} - Q_{\text{Surr}} \quad (1)$$

where m and C_p are the mass (0.2 g) and heat capacity (4.2 J/g) of water, respectively, and T represents the solution temperature, Q_{Material} stands for the energy generated by the material ($Ti_3C_2T_x$ or $Au_y@Ti_3C_2T_x$) during the irradiation of 660 nm laser, Q_{Dis} is the baseline energy generated by the container and pure water under the same irradiation condition, and Q_{Surr} is the dissipated energy as heat into the surroundings.

For the energy input term, Q_{Material} can be written as

$$Q_{\text{Material}} = I(1-10^{-A_{660}})\eta \quad (2)$$

in which I stands for the power of the incident beam with unit mW, A_{660} represents the absorbance of the $Ti_3C_2T_x$ or $Au_y@Ti_3C_2T_x$ at 660 nm, and η is the photothermal conversion efficiency from incident light to dissipated heat.

For the energy output term, Q_{Surr} can be calculated by the following equation:

$$Q_{\text{Surr}} = hS(T - T_{\text{Surr}}) \quad (3)$$

where h is the heat transfer coefficient, S is the surface area of the container, and T_{Surr} is the environment temperature.

Once the incident laser is settled, the total energy input will be finite, while the energy output increases as the solution temperature increases. However, a dynamic equilibrium will be achieved as the solution energy reaches a maximum (T_{Max}) when the energy input terms ($Q_{\text{Material}} + Q_{\text{Dis}}$) balance the energy output term $(Q_{\text{Surr}})_{\text{Max}}$.

$$Q_{\text{Material}} + Q_{\text{Dis}} = (Q_{\text{Surr}})_{\text{Max}} = hS(T_{\text{Max}} - T_{\text{Surr}}) \quad (4)$$

To get the equation (5) typically used to calculate the photothermal conversion efficiency (η), equation (2) was substituted into (4):

$$\eta = \frac{hS(T_{\text{Max}} - T_{\text{Surr}}) - Q_{\text{Dis}}}{I(1-10^{-A_{660}})} \quad (5)$$

Since h and S are hard to be measured or calculated directly, a conventional method is adopted by utilizing data from the cooling period, in which a dimensionless

driving force (θ) is introduced. θ can be expressed in terms of T_{Max}:

$$\theta = \frac{T - T_{Surr}}{T_{Max} - T_{Surr}} \tag{6}$$

The time constant (τ_s) of the sample system is defined as:

$$\tau_s = \frac{\sum_i m_i C_{p,i}}{hS} \tag{7}$$

Then, equation (6) and (7) are substituted into (1) to get the following equation:

$$\frac{d\theta}{dt} = \frac{1}{\tau_s}\left[\frac{Q_{Material} + Q_{Dis}}{hS(T_{Max} - T_{Surr})} - \theta\right] \tag{8}$$

During the cooling period, when no light (external energy) is applied, there is no energy input ($Q_{Material} + Q_{Dis} = 0$). Therefore, equation (8) can be further simplified to:

$$dt = -\tau_s \frac{d\theta}{\theta} \tag{9}$$

and integration gives:

$$t = -\tau_s ln\theta \tag{10}$$

According to equation (10), by plotting *t vs.* -lnθ, the following τ_s values are obtained: 275.32 s for the $Ti_3C_2T_x$ NSs (Figure S11) and 233.91 s for the $Au_{0.017}$@$Ti_3C_2T_x$ (Figure 4c), respectively, with corresponding A_{660} values of 0.848 and 1.298. Therefore, the photothermal conversion efficiency was calculated to be 33.52 % for the $Ti_3C_2T_x$ and 47.93 % for $Au_{0.017}$@$Ti_3C_2T_x$.

References

1. D. K. Roper, W. Ahn and M. Hoepfner, *J. Phys. Chem. C*, 2007, **111**, 3636-3641.